Article

Not peer-reviewed version

Regularities of Metal Transfer by Nickel-Based Superalloy Tool at Friction Stir Processing of Titanium Alloy, Produced by Wire Feed Electron Beam Additive Manufacturing

Valery Rubtsov , Andrey Chumaevskii * , Evgeny Knyazhev , Veronika Utyaganova , Denis Gurianov , Alihan Amirov , Andrey Cheremnov , Evgeny Kolubaev

Posted Date: 21 November 2023

doi: 10.20944/preprints202311.1297.v1

Keywords: friction stir processing; additive manufacturing; wire; titanium alloy; material transfer; microstructure; microhardness

Article

Regularities of Metal Transfer by Nickel-Based Superalloy Tool at Friction Stir Processing of Titanium Alloy, Produced by Wire Feed Electron Beam Additive Manufacturing

Valery Rubtsov, Andrey Chumaevskii *, Evgeny Knyazhev, Veronika Utyaganova, Denis Gurianov, Alikhan Amirov, Andrey Cheremnov and Evgeny Kolubaev

Institute of Strength Physics and Materials Science, Siberian Branch of Russian Academy of Sciences, 634055, Tomsk, Russian Federation; rvy@ispms.ru; tch7av@ispms.ru; clothoid@ispms.ru; filaret_2012@mail.ru; gurianov@ispms.ru; amc@ispms.ru

* Correspondence: tch7av@ispms.ru

Abstract: In this work, the interaction of additively produced Ti64 titanium alloy with a nickel superalloy tool and the features of the stir zone formation during friction stir processing have been studied. The stop-action technique was used to produce the samples to be studied using optical and scanning electron microscopy methods, as well as microhardness measurements. As a result, it was revealed that the tool, when moving, forms a pre-deformed area in front of it, which is characterized by a fine-grained structure. The presence of an interface layer of the workpiece material primary fragmentation by the tool was revealed. It was demonstrated that the transfer of titanium alloy material occurs periodically following the ratio of feeding speed to tool rotation rate.

Keywords: friction stir processing; additive manufacturing; wire; titanium alloy; material transfer; microstructure; microhardness

1. Introduction

Friction stir welding and processing (FSW/P) of titanium alloys is currently becoming an increasingly important and frequently used technology. This is explained by the fact that titanium alloys remain the most used in many industries, ranging from the production of mobile device bodies to aerospace components [1–3]. In addition, the growing demand for additive technologies is also contributing to the increasing popularity of FSW/P of titanium alloys, as the challenge of improving the structure and mechanical properties of additive products is now acute [4–6]. This problem is most serious in the case of directed energy deposition methods to produce large-sized titanium alloy products [7]. This is primarily caused by the complex thermal cycles in the 3D printing process that led to the formation of a directionally oriented coarse-grained structure [8,9]. In the case of titanium alloys, the structure is represented by columnar grains of the primary β phase, and the length of these grains can reach several centimeters [10]. At the same time, the size and morphology of the α and α' phase plates, which fill the columnar grains, change with the growth of the additive product wall due to changes in the heat dissipation conditions [11]. The above features lead to a high anisotropy of both the structure and mechanical characteristics of the titanium alloy material [12]. Moreover, the properties of additive alloys in this case are significantly inferior to the required values [13]. In turn, friction stir processing, which allows modifying the structure of both the surface and the volume of the product due to dynamic recrystallization, can be used to locally improve the characteristics of additive parts and has already shown positive results both in the processing of aluminum alloys [14,15] and titanium alloys [16,17]. However, in the case of titanium alloys, the process of the stir zone formation by FSW/P and the peculiarities of material flow are still under-explored.

 doi:10.20944/preprints202311.1297.v1

The stop-action technique [18] is the most suitable for studying the deformation peculiarities and the material structure formation in the FSW-tool effect zone. It allows to simultaneously study both the structure of the workpiece and the features of tool wear during FSW/P and has found its application even in the field of steel welding [19]. This method consists of abruptly interrupting the welding/processing process so that the tool remains in the body of the welded workpiece. The resulting sample is then cut into sections and the structure of the workpiece around the tool is examined. This approach also provides an opportunity to evaluate the fragmentation and adhesion transfer features of the material during FSW/P, as shown in [20]. This will help to better understand the nature of the titanium alloy interaction with the tool and the formation of the stir zone. Thus, the purpose of this work is to study the material structure of additive Ti64 alloy in the zone of tool influence using the stop-action technique and to identify the features of the stir zone formation during friction stir processing.

2. Materials and Methods

To study the peculiarities of the stir zone formation, samples of wall-shaped workpieces made of Ti64 titanium alloy were produced by the wire-feed electron beam additive manufacturing method. 3D printing was performed on a self-developed wire-feed EBAM machine at the Institute of Strength Physics and Materials Science, Tomsk, Russia. The workpieces in as-built condition had dimensions of 300 mm in height, 100 mm in length, and 6 mm in width. Before friction stir processing, 2.5 mm thick plates were cut out of these blanks by EDM-machine DK7750 (Suzhou Simos CNC Technology Co., Ltd., Suzhou, China) similar to the scheme presented in [17]. After that, friction stir processing was performed on a homemade friction stir welding machine using the following parameters: loading force 33.34 kN, tool travel speed 90 mm/min, and tool rotation rate 400 rpm. The workpieces were processed in two directions: vertical (along the wall growth direction) and horizontal (along the layer deposition direction). During the processing, an interruption was performed so that the tool remained in the workpiece according to the stop-action technique. Then the obtained sample was sectioned using EDM-machine DK7750 according to the scheme shown in Figure 1.

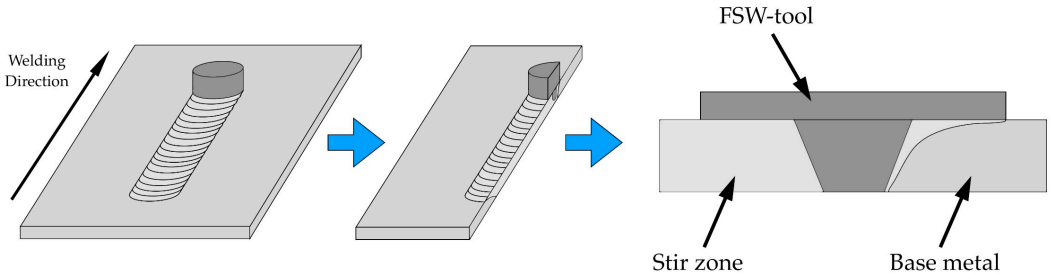

Figure 1. Schematic illustration of sample cutting

The resulting sections were mechanically ground, polished, and chemically etched to study the structure of the material. The structure was analyzed using the Altami MET-1C optical microscope (Altami Ltd., Saint Petersburg, Russia). In addition, studies were carried out using scanning electron microscopy for finer microstructure and elemental analysis. For this purpose, the Apreo 2 S LoVac scanning electron microscope (Thermo Fisher Scientific Inc., Waltham, MA, USA) was used. The microhardness of the material was measured in a longitudinal section with a load of 0.5 kg and an increment of 0.5 mm. Duramin 5 microhardness tester (Struers A/S, Ballerup, Denmark) was used for this procedure.

3. Results

As a result of the experiments, two samples with the tool remaining in the workpiece after processing in the horizontal and vertical directions were prepared. First, the macrostructure of the samples was investigated (Figure 2). The specimens showed a distinct pre-deformed area (PDA) in

Preprints (www.preprints.org) | NOT PEER-REVIEWED | Posted: 21 November 2023 doi:10.20944/preprints202311.1297.v1

the region in front of the tool, which borders the base metal. Light-colored interfaces are identified on the tool predominantly in the lower half of the pin, but they are also observed in the area under the tool shoulders on the stir zone side (SZ, Figure 2, b). The shape of this surface layer in the horizontal sample, as well as the shape of the worn tool in combination with the visible torn-off and mixed into the stir zone surface layer in the vertical sample, may indicate that the formation of this layer is one of the mechanisms of tool wear during FSW/P of titanium alloys. This can also be evidenced by the periodic mixing of this material in the SZ, which is observed in the lower part of the workpiece. It should be noted that in the vertical sample, the tool was worn more intensively, and therefore the stirring of the interface layer in the SZ was also more intense compared to the horizontal sample.

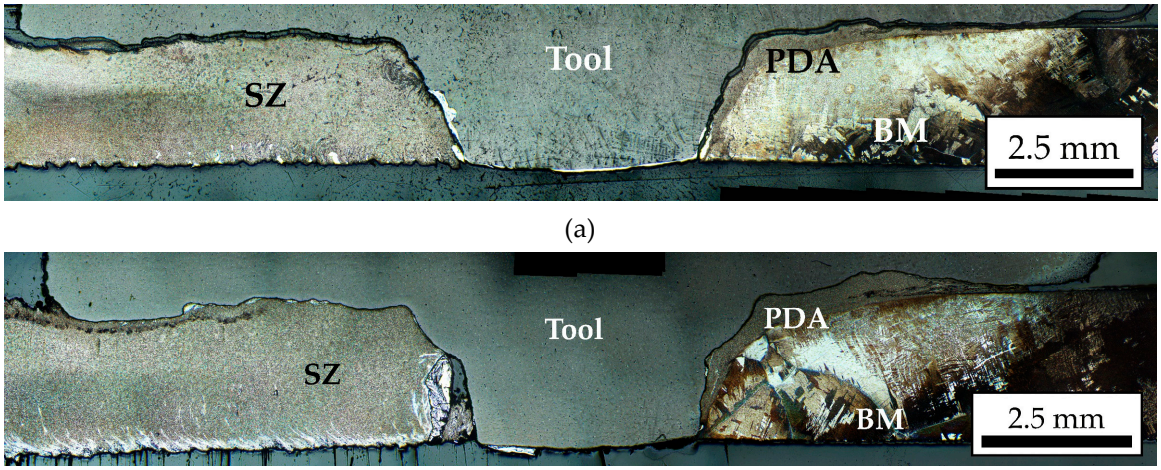

Figure 2. Macroscopic images of samples produced by stopping FSP process when processing along horizontal (a) and vertical (b) direction. SZ – stir zone, PDA – pre-deformed area, BM – base metal.

Figure 3 shows images of the microstructure of the sample produced by processing in the horizontal direction. The microstructure of the base metal (Figure 3, a) presents a typical structure for additive material and represents grains of primary β phase separated by grain-boundary α phase (α-GB). Inside these grains are large colonies of alpha phase plates. After processing, due to severe plastic deformation and dynamic recrystallization, the structure of the material changes from lamellar to globular with small almost equiaxed grains in the stir zone (Figure 3, c). Of greatest interest is the pre-deformed area in the region in front of the tool (Figure 3, b). Its dimensions are of the order of 200 μm and vary with the height of the workpiece. The greatest width of the pre-deformed area is observed in the transition zone from the shoulder part of the tool to the pin, i.e., where the strongest tangential stresses during machining occur [21]. The interface layer observed in the macro-images at different parts of the sample has different sizes and predominantly has a layered structure due to the high deformation degree at FSP (Figure 3, c). The largest proportion of this layer is concentrated in the lower part of the pin on the side behind the tool.

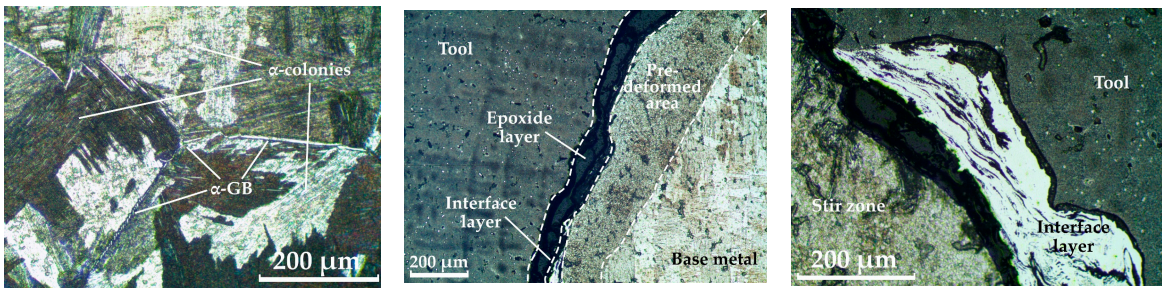

Preprints (www.preprints.org) | NOT PEER-REVIEWED | Posted: 21 November 2023 doi:10.20944/preprints202311.1297.v1

Figure 3. Metallography images of the base metal (a), area in front of the tool (b), and area behind the tool (c) in the sample produced along horizontal direction. GB – grain boundary.

In the sample produced by processing in the vertical direction, the structure is formed similarly. The base metal is also represented by primary β phase grains and α colonies (Figure 4, a), and the stir zone is represented by small recrystallized α grains (Figure 4, c). However, in contrast to the horizontal sample, the interface layer between the tool and the workpiece has a longer extent and in addition to the layered structure, it also has a fragmented structure (Figure 4, c). The average grain size is about 4.9 ± 1.5 μm. The size of the transition zone is similar to the previous example, but since the tool is more worn here, in the pre-deformed area there are inclusions of surface layer particles displaced as a result of tool wear during processing (Figure 4, b). The grain size in the pre-deformed area is smaller than in the stir zone and is 3.3 ± 1.4 μm, which is also confirmed by the darker etching in the macro-image due to the higher density of grain boundaries.

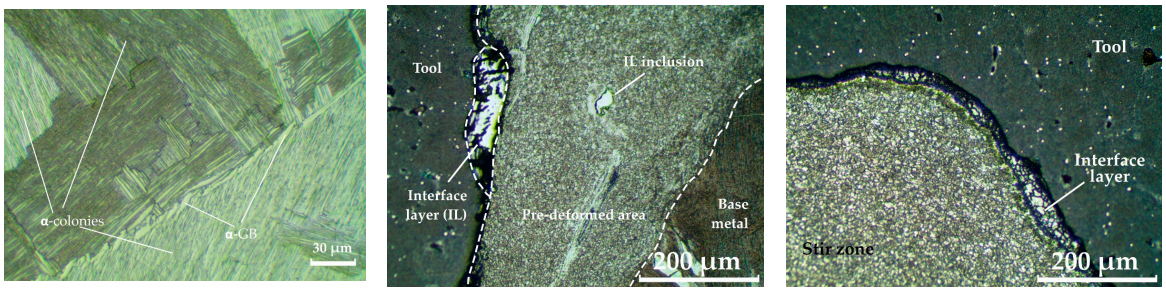

(a) (b) (c)

Figure 4. Metallography images of the base metal (a), area in front of the tool (b), and area behind the tool (c) in the sample produced along vertical direction. GB – grain boundary.

Microhardness measurement shows that the pre-deformed region shows the maximum value of microhardness in each of the samples, and even exceeds the tool hardness (Figure 4, a, b). At the same time, it is worth noting that the microhardness in the stir zone is slightly lower than in the base metal.

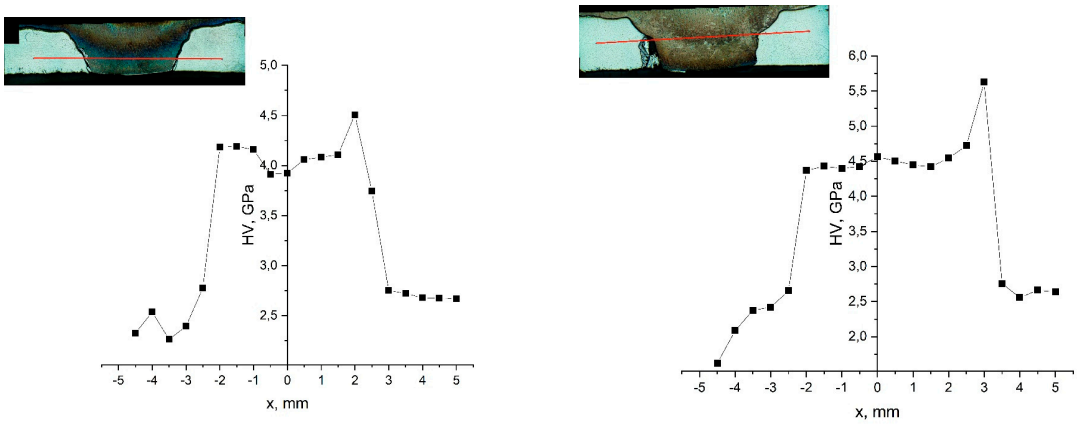

(a) (b)

Figure 4. Vickers microhardness (HV) of samples produced in horizontal (a) and vertical (b) direction.

Scanning electron microscopy was used to study the surface layer in different parts of the tool, including measurements of the chemical composition of this layer. It was revealed that the coarse layers in the lower part of the tool and the continuous layers in the middle of the pin and under the shoulders are different. The first type of interface layer (Figure 5) is a continuous layer formed as a result of the interaction between the tool and the workpiece. As the analysis of chemical composition shows, this layer is based on titanium alloy (76% Ti, 6.5% Al, 3.3% V) with the inclusion of elements

Preprints (www.preprints.org) | NOT PEER-REVIEWED | Posted: 21 November 2023 doi:10.20944/preprints202311.1297.v1

of the tool material (9.4% Ni, 2.3% Cr, 1.6% Co, and 0.9% W). Thus, it can be concluded that this layer is formed as a result of diffusion of nickel alloy elements into the workpiece material, probably in the process of adhesion-diffusion wear of the tool. As for the structure of this layer, the image in Figure 5, a show that this layer is fragmented into small cells near the tool and larger cells in the area of contact with the workpiece material (1). There is a clear boundary between the surface layer and the stir zone (2). In the area near the boundary, there are also traces of further fragmentation deep into the workpiece (3).

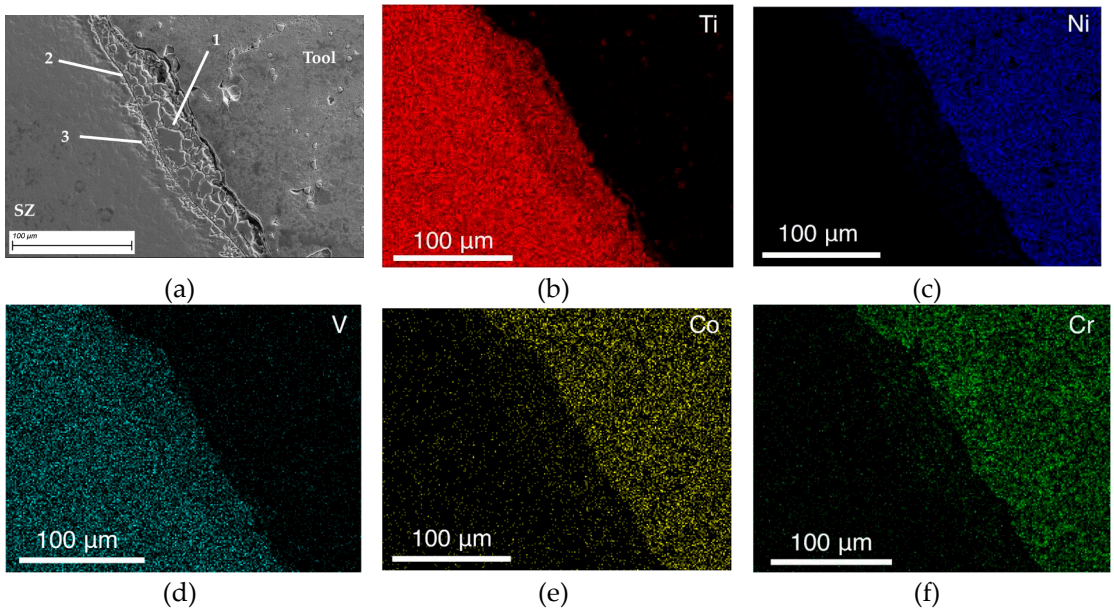

Figure 5. SEM-image of the first type of interlayer between tool and stir zone (a) and maps of the chemical element distribution (b – f).

The second type of interface layer, which is observed predominantly at the bottom of the tool and mixed at the bottom of the stir zone, is shown in Figure 6. Chemical analysis shows that the material of this layer is not related to either the workpiece material or the tool. The chemical element distribution maps (Figure 6, d - f) showed that this layer is chromium-nickel steel. Thus, the tool may have encountered the substrate during the welding/processing operation. Although this is not the correct course of the FSP process, it allows us to demonstrate the adhesive nature of the stir zone formation using steel as a marker material. First, the steel material is captured by the bottom plane of the pin and is carried upward, reaching the middle of the pin along the side (Figure 2). Then, as the tool rotates and moves, this layer is detached from the pin and mixed into the workpiece material. The material transfer process is periodic but irregular, as can be seen in Figure 2.

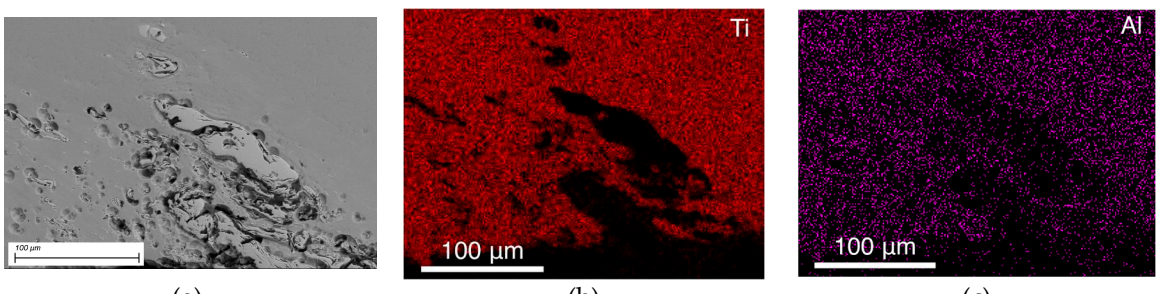

Preprints (www.preprints.org) | NOT PEER-REVIEWED | Posted: 21 November 2023 doi:10.20944/preprints202311.1297.v1

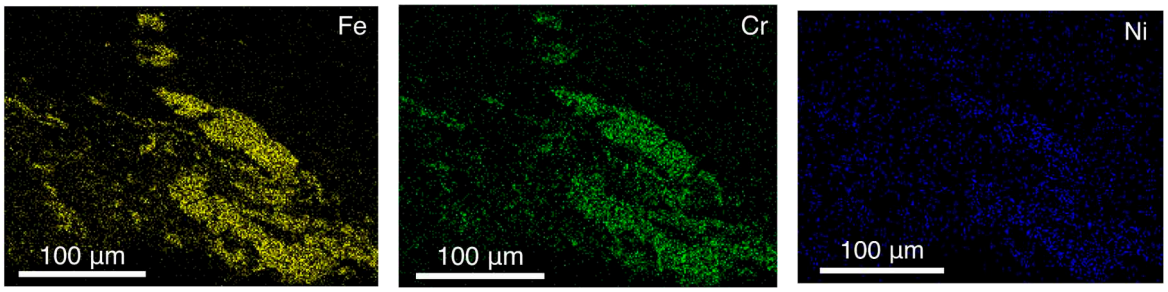

(d) (e) (f)

Figure 6. SEM-image of the second type of interlayer mixed into the stir zone (a) and maps of the chemical element distribution (b – f).

4. Discussion

Studies have shown that the tool during friction stir processing significantly deforms the material in front of it while moving. As the analysis of the material micro-structure showed, the size of the pre-deformed area is about 200 microns, and the grain size in it is on average 3.3 µm. When the material is transferred to the zone behind the tool, i.e. forms the stir zone, the material structure recrystallizes, as a result of which the grain size in the stir zone increases and averages 4.9 µm. At the same time in the contact zone of the tool with the workpiece, there is a layer of material, representing a titanium alloy with a small share of chemical elements of the tool material. Based on the structure of this layer (Figures 4 and 5), it could be formed because of the primary fragmentation of the material, i.e., at the initial stage of the transfer layer formation [20]. From the data obtained, it can be concluded that, as a result of thermomechanical action, the tool fragments a material layer up to 30 µm thick, depending on the tool section and the stresses in this section. Part of this layer eventually forms a transfer layer, while another part recrystallizes with the pre-deformed area material.

Once the transfer layer reaches a critical size, it is adhered to the tool and transferred to the area behind the tool [22]. By stirring a foreign material (stainless steel), it was possible to trace the material transfer pattern during friction stir processing of titanium alloy. It is known that an approximate estimate of the thickness of the transferred layers can be made through the ratio of the tool feeding speed to the tool rotation rate [23]. In this case, at a travel speed of 90 mm/min and a rotation rate of 400 rpm, the tool passes 0.225 mm per rotation. Consequently, the tool can transfer a material layer with a thickness of about 0.225 mm per revolution. Using optical metallography images, the distances between the mixed layers of steel were measured (Figure 7).

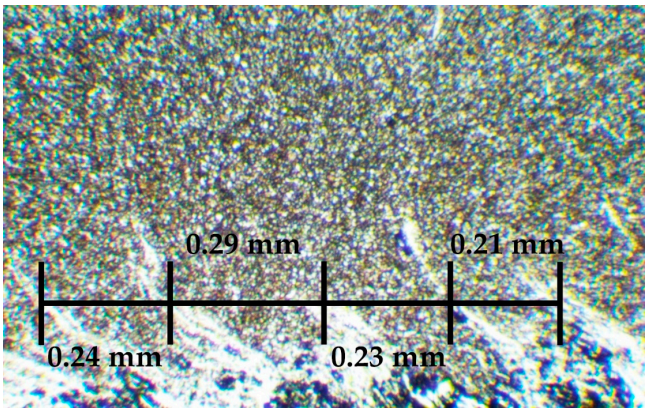

Figure 7. Microscopic image illustrating the pattern of material stirring with distances between intermixed layers.

The measurements showed that the distance between the layers of the steel mixed into the stir zone is about 0.24 ± 0.034 mm. Therefore, since stainless steel acts as a marker material, it can be stated that the thickness of the transferred layers is almost equal to the calculated value of tool travel per

rotation. Consequently, for titanium alloys, the regularities that have been determined for welding aluminum alloys [23] are valid both in terms of material fragmentation and formation of transfer layers and in terms of the regularities of the stir zone formation depending on the process parameters.

5. Conclusions

The following conclusions have thus been drawn from the research conducted.

1. During friction stir processing of additive Ti64 titanium alloy, a wide zone of pre-deformed material is formed in the zone in front of the tool, which is characterized by finer grains than in the stir zone. When the material is transferred behind the tool, the grain size increases due to recrystallization.
2. An interface layer is formed between the tool and the workpiece, which is a layer of primary fragmented material characterized by diffusion of chemical elements of the tool material into the body of the workpiece.
3. When the tool contacts the substrate, the substrate material is transferred from the bottom to the top and mixed into the stir zone of the titanium alloy. This material forms a layer between the tool and the workpiece and increases tool wear.
4. The frequency of material transfer during friction stir processing of titanium alloy is determined by the ratio of the tool feeding speed to its rotation rate, similar to aluminum alloys.

Author Contributions: Conceptualization, V.R. and A.C. (Chumaevskii); methodology, A.C. (Chumaevskii); investigation, E.K., V.U., D.G. and A.C. (Cheremnov); resources, A.C. (Chumaevskii); data curation, A.C. (Cheremnov); writing—original draft preparation, A.C. (Chumaevskii); writing—review and editing, V.R.; visualization, E.K., V.U., D.G. and A.C. (Cheremnov); project administration, V.R.; funding acquisition, V.R. All authors have read and agreed to the published version of the manuscript.

Funding: This research project was supported by the Russian Science Foundation under grant No 22-29-20172, https://rscf.ru/en/project/22-29-20172/ (accessed on 11 November 2023) and funded by the Administration of the Tomsk Region.

Conflicts of Interest: The authors declare no conflict of interest.

References

1. Kallee, S.W. 5 - Industrial Applications of Friction Stir Welding. In Friction Stir Welding; Lohwasser, D., Chen, Z., Eds.; Woodhead Publishing Series in Welding and Other Joining Technologies; Woodhead Publishing, 2010; pp. 118–163 ISBN 978-1-84569-450-0.
2. Longhurst, W.R.; Cox, C.D.; Gibson, B.T.; Cook, G.E.; Strauss, A.M.; Wilbur, I.C.; Osborne, B.E. Development of Friction Stir Welding Technologies for In-Space Manufacturing. *Int. J. Adv. Manuf. Technol.* **2017**, 90, 81–91, doi:10.1007/s00170-016-9362-1.
3. Burford, D.; Widener, C.; Tweedy, B. Advances in Friction Stir Welding for Aerospace Applications. In Proceedings of the 6th AIAA Aviation Technology, Integration and Operations Conference (ATIO); American Institute of Aeronautics and Astronautics: Reston, Virigina, September 25, 2006.
4. Liu, H.J.; Zhou, L.; Huang, Y.X.; Liu, Q.W. Study of the Key Issues of Friction Stir Welding of Titanium Alloy. *Mater. Sci. Forum* **2010**, 638–642, 1185–1190, 10.4028/www.scientific.net/MSF.638-642.1185.
5. Nguyen, H.D.; Pramanik, A.; Basak, A.K.; Dong, Y.; Prakash, C.; Debnath, S.; Shankar, S.; Jawahir, I.S.; Dixit, S.; Buddhi, D. A Critical Review on Additive Manufacturing of Ti-6Al-4V Alloy: Microstructure and Mechanical Properties. *J. Mater. Res. Technol.* **2022**, 18, 4641–4661, https://doi.org/10.1016/j.jmrt.2022.04.055.
6. Hrabe, N.; Gnäupel-Herold, T.; Quinn, T. Fatigue Properties of a Titanium Alloy (Ti–6Al–4V) Fabricated via Electron Beam Melting (EBM): Effects of Internal Defects and Residual Stress. *Int. J. Fatigue* **2017**, 94, 202–210, https://doi.org/10.1016/j.ijfatigue.2016.04.022.
7. Carroll, B.E.; Palmer, T.A.; Beese, A.M. Anisotropic Tensile Behavior of Ti–6Al–4V Components Fabricated with Directed Energy Deposition Additive Manufacturing. *Acta Mater.* **2015**, 87, 309–320, https://doi.org/10.1016/j.actamat.2014.12.054.
8. Lopez-Castaño, S.; Emile, P.; Archambeau, C.; Pettinari-Sturmel, F.; Douin, J. Main Microstructural Characteristics of Ti-6Al-4V Components Produced via Electron Beam Additive Manufacturing (EBAM) BT - TMS 2021 150th Annual Meeting & Exhibition Supplemental Proceedings.; Springer International Publishing: Cham, 2021; pp. 176–188.
9. Manjunath, A.; Anandakrishnan, V.; Ramachandra, S.; Parthiban, K.; Sathish, S. Investigations on the Effect of Build Orientation on the Properties of Wire Electron Beam Additive Manufactured Ti-6Al-4V Alloy. *Mater. Today Commun.* **2022**, 33, 104204, https://doi.org/10.1016/j.mtcomm.2022.104204.

10. Kalashnikov, K.N.; Chumaevskii, A. V; Kalashnikova, T.A.; Osipovich, K.S.; Kolubaev, E.A. Defect Formation in Titanium Alloy during Non-Stationary Process of Local Metallurgy. *Russ. Phys. J.* **2020**, 63, 962–967, doi:10.1007/s11182-020-02124-1.
11. Kalashnikov, K.N.; Chumaevskii, A.V.; Kalashnikova, T.A.; Kolubaev, E.A. A Substrate Material and Thickness Influence on the 3D-Printing of Ti–6Al–4V Components via Wire-Feed Electron Beam Additive Manufacturing. *J. Mater. Res. Technol.* **2022**, 16, 840–852, doi:10.1016/j.jmrt.2021.12.024.
12. Hoefer, K.; Nitsche, A.; Haelsig, A.; Mayr, P. Manufacturing of Titanium Components with 3DPMD. *Metals (Basel)*. **2019**, 9, 562, doi:10.3390/met9050562.
13. Baufeld, B.; Brandl, E.; van der Biest, O. Wire Based Additive Layer Manufacturing: Comparison of Microstructure and Mechanical Properties of Ti–6Al–4V Components Fabricated by Laser-Beam Deposition and Shaped Metal Deposition. *J. Mater. Process. Technol.* **2011**, 211, 1146–1158, https://doi.org/10.1016/j.jmatprotec.2011.01.018.
14. Rafieazad, M.; Mohammadi, M.; Gerlich, A.; Nasiri, A. Enhancing the Corrosion Properties of Additively Manufactured AlSi10Mg Using Friction Stir Processing. *Corros. Sci.* **2021**, 178, 109073, https://doi.org/10.1016/j.corsci.2020.109073.
15. Yang, T.; Wang, K.; Wang, W.; Peng, P.; Huang, L.; Qiao, K.; Jin, Y. Effect of Friction Stir Processing on Microstructure and Mechanical Properties of AlSi10Mg Aluminum Alloy Produced by Selective Laser Melting. *JOM* **2019**, 71, 1737–1747, doi:10.1007/s11837-019-03343-9.
16. Kalashnikova, T.; Cheremnov, A.; Eliseev, A.; Gurianov, D.; Knyazhev, E.; Moskvichev, E.; Beloborodov, V.; Chumaevskii, A.; Zykova, A.; Kalashnikov, K. Structural Changes in Block-Shaped WEBAM'ed Ti6Al4V Samples after Friction Stir Processing. *Lubricants* **2022**, 10, 349, doi:10.3390/lubricants10120349.
17. Kalashnikov, K.; Chumaevskii, A.; Kalashnikova, T.; Cheremnov, A.; Moskvichev, E.; Amirov, A.; Krasnoveikin, V.; Kolubaev, E. Friction Stir Processing of Additively Manufactured Ti-6Al-4V Alloy: Structure Modification and Mechanical Properties. *Metals (Basel).* **2021**, 12, 55, doi:10.3390/met12010055.
18. Kalinenko, A.; Dolzhenko, P.; Malopheyev, S.; Shishov, I.; Mishin, V.; Mironov, S.; Kaibyshev, R. Microstructural Evolution and Material Flow during Friction Stir Welding of 6013 Aluminum Alloy Studied by the Stop-Action Technique. *Metals (Basel).* **2023**, 13, 1342, doi:10.3390/met13081342.
19. Pfeiffer, C.; Weinberger, T.; Schröttner, H.; Mitsche, S.; Enzinger, N. Investigation of Friction Stir Welding of Stainless Steel Using a Stop-Action-Technique. In Proceedings of the THERMEC 2011 Supplement; Trans Tech Publications Ltd, 2012; Vol. 409, pp. 293–298.
20. Kalashnikova, T.; Chumaevskii, A.; Kalashnikov, K.; Fortuna, S.; Kolubaev, E.; Tarasov, S. Microstructural Analysis of Friction Stir Butt Welded Al-Mg-Sc-Zr Alloy Heavy Gauge Sheets. *Metals (Basel).* **2020**, 10, 806, doi:10.3390/met10060806.
21. Tarasov, S.Y.; Rubtsov, V.E.; Kolubaev, E.A. A Proposed Diffusion-Controlled Wear Mechanism of Alloy Steel Friction Stir Welding (FSW) Tools Used on an Aluminum Alloy. *Wear* **2014**, 318, 130–134, https://doi.org/10.1016/j.wear.2014.06.014.
22. Tarasov, S.Y.; Filippov, A. V; Kolubaev, E.A.; Kalashnikova, T.A. Adhesion Transfer in Sliding a Steel Ball against an Aluminum Alloy. *Tribol. Int.* **2017**, 115, 191–198, https://doi.org/10.1016/j.triboint.2017.05.039.
23. Eliseev, A.A.; Kalashnikova, T.A.; Filippov, A. V; Kolubaev, E.A. Material Transfer by Friction Stir Processing. In Multiscale Biomechanics and Tribology of Inorganic and Organic Systems: In memory of Professor Sergey Psakhie; Ostermeyer, G.-P., Popov, V.L., Shilko, E. V, Vasiljeva, O.S., Eds.; Springer International Publishing: Cham, 2021; pp. 169–188 ISBN 978-3-030-60124-9.